



# Water-insoluble, nanocrystalline, and hydrogel fibrillar scaffolds for biomedical applications

Dong-Hee Kang<sup>1</sup> · Dongyoon Kim<sup>1</sup> · Sungrok Wang<sup>1</sup> · Dasom Song<sup>1</sup> · Myung-Han Yoon<sup>1</sup>

Received: 31 January 2018 / Revised: 14 March 2018 / Accepted: 16 March 2018 / Published online: 26 April 2018  
© The Society of Polymer Science, Japan 2018

## Abstract

Recently, micro/nanofibrillar materials have been widely utilized for a variety of applications in many different fields of research due to their relatively large surface-to-volume ratios, high porosity, and three-dimensional connectivity, along with their cost-effective fabrication processes. Herein, we present a review of recent progress in the development of micro/nanofibrillar scaffolds with a specific focus on their biomedical applications. From the perspective of controlling polymer–polymer and polymer–water molecular interactions, we categorized the fibrillar scaffolds into insoluble, nanocrystalline, and hydrogel fibers. Based on our recent studies related to this research topic, we provide the significance and essential information on four different micro/nanofibrillar scaffolds: (1) solid micro/nanofibrillar scaffolds based on water-insoluble polymers, (2) hydrogel nanofibrillar network scaffolds based on crystalline bacterial cellulose, (3) hydrogel micro/nanofiber scaffolds based on partially precipitated PVA, and (4) hydrogel micro/nanofiber scaffolds based on chemically cross-linked PVA. The present discussion should provide guidance to researchers in selecting a micro/nanofibrillar scaffold suitable for their own purposes and should help inspire them to develop more sophisticated fibrillar scaffolds in the future.

## Introduction

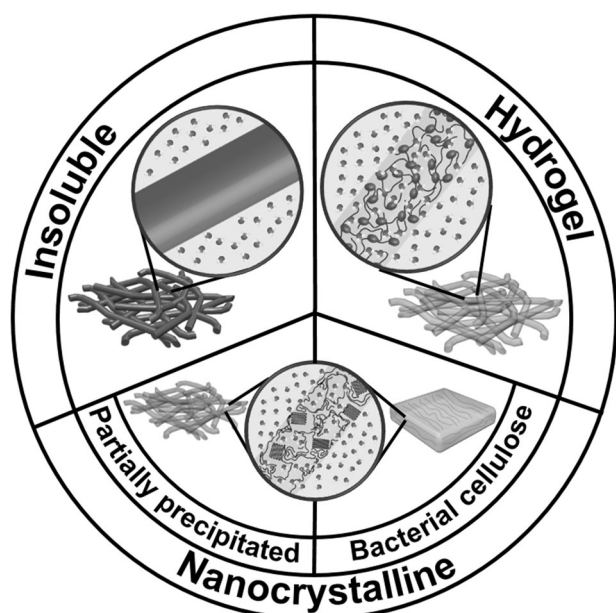
Over the past several decades, fibrillar materials have been widely utilized for a variety of applications in the fields of energy conversion/storage and environmental and biomedical engineering because of their unique structures, cost-effective fabrication processes, and constituent material properties. In particular, their relatively large surface-to-volume ratios, high porosity, and three-dimensional (3D) connectivity increase the effective surface areas and promote chemical diffusion through the porous structures. Consequently, these beneficial properties of fibrillary structures enable improved device performance and lifetime in many energy conversion/storage devices [1–6], enhanced removal efficiency of pollutants in both water and air filtration systems [7–10], and 3D cell cultures emulated the *in vivo* tissue environment [11–16].

Several well-known methods, such as electrospinning, melt-blowing, and self-assembly [17–19], have been successfully employed to fabricate micro/nanofibrillar scaffolds for various biomedical applications. Until recently, the vast majority of previous reports have focused on the functional and/or geometrical modifications of fibrillar scaffolds by applying specific surface treatments, incorporating additional materials, or adjusting fibrillation processes. For example, porous, hollow, flattened, and branched fibrillar structures have been developed by controlling the conditions for fiber formation and/or employing post-processing on as-prepared fibrillar structures [20–22]. In particular, porous biocompatible scaffolds, which contain a substantial number of microscale voids (10–100 μm) and permit favorable cell migration/penetration, have been intensively utilized in tissue engineering and related fields [23–25]. It has been reported that 3D cell cultures constructed with scaffold materials mimicking the porous structure of the extracellular matrix (ECM) not only exhibit good cell viability but also emulate many *in vivo* characteristics of the

These authors contributed equally: Dong-Hee Kang, Dongyoon Kim.

✉ Myung-Han Yoon  
mhyoon@gist.ac.kr

<sup>1</sup> School of Materials Science and Engineering, Gwangju Institute of Science and Technology, 123 Cheomdangwagi-ro, Buk-gu, Gwangju 500712, Republic of Korea



**Scheme 1** A schematic diagram showing three different types of micro/nanofibrillar scaffolds depending on polymer–polymer and polymer–water molecular interactions: insoluble, nanocrystalline (bacterial cellulose and partially precipitated), and hydrogel

biological tissue [26, 27]. It is also noteworthy that in addition to the void fraction (i.e., porosity), topological factors are important in determining the extracellular/cellular network connectivity and the corresponding scaffold functions [28, 29].

In parallel to micro/nanofibrillar scaffolds, several different types of hydrogel materials have been developed as alternative biomedical platforms for tissue engineering and drug delivery [30, 31]. A hydrogel is a transparent 3D network composed of hydrophilic natural or synthetic polymers, in which a large amount of water content is retained, and the resultant structural and mechanical properties can be easily adjusted in a similar manner as those of the real ECM, leading to extensive applications of hydrogels in the field of biomedical engineering [32, 33]. In particular, various hydrogels have been successfully utilized to investigate mechanotransduction in mammalian cells by monitoring the behaviors of cells grown on them while delicately monitoring the physical and chemical properties of the hydrogel [34, 35]. Compared to solid fibrillar scaffolds, hydrogels contain relatively small pores (1–10 nm) [36, 37] due to the dense polymer network formed by cross-linking, which sometimes limits molecular diffusion and active transport through the hydrogel matrix despite their much higher optical transparency [38, 39]. Although hydrogels derived from natural materials, for instance, collagen gel and Matrigel, have been frequently utilized for mimicking the properties of the ECM *in vivo* [40, 41], the limited diffusion of biomolecules into/out of these

materials, the inclusion of unknown biological factors, the gradual degradation and resultant property changes, and the relatively high material cost prevent their widespread usage for various biological and biomedical studies [42, 43]. Therefore, it would be desirable to prepare novel fibrillar scaffolds that contain the characteristics of both solid micro/nanofibers and hydrogels simultaneously in a controlled manner for a specific application.

In this article, we present a review of recent progress in the development of micro/nanofibrillar scaffolds with a specific focus on their biomedical applications. Special emphasis was placed on the classification of fibrillar scaffolds into three categories (insoluble, nanocrystalline, and hydrogel fibers (Scheme 1)) according to their aqueous solubility, crystallinity, and swelling, which are caused by specific polymer–polymer and polymer–water interactions. More specifically, four different fibrillar scaffolds recently studied by our research group are mainly reviewed: (1) solid micro/nanofibrillar scaffolds based on water-insoluble polymers, (2) hydrogel nanofibrillar network scaffolds based on crystalline bacterial cellulose (BC), (3) hydrogel micro/nanofiber scaffolds based on partially precipitated poly(vinyl alcohol) (PVA), and (4) hydrogel micro/nanofiber scaffolds based on chemically cross-linked PVA. The corresponding characteristics, such as composition, controllability, fiber stiffness, and transparency, are summarized in Table 1. It is also important to control the surface chemical functionality of scaffold materials according to the cultured cell type (e.g., neuron), which has been well described elsewhere [44], but in this article, we mainly focus on highlighting the importance of hydrogel micro/nanofibrillar structures and the microscale porosity within the scaffold by showing related experimental results we obtained recently.

### Solid micro/nanofibrillar scaffolds based on water-insoluble polymers

Typical polymeric fibers are mainly formed using water-insoluble polymers such as polycaprolactone (PCL) [45], polystyrene (PS) [26, 46, 47], polysulfone [8, 48], poly(vinylidene fluoride) [49, 50], and polyacrylonitrile [51]. These fibers have been well studied for various environmental and energy conversion/storage applications because they can be easily fabricated from solution of these polymers in common organic solvents and because they exhibit high porosity and large surface-to-volume ratios [6, 52]. Furthermore, since most of these polymers also show minimal solubility in water, van der Waals interactions among polymeric chains inside solid fibers are marginally perturbed by water molecules. Therefore, the stability in the biological environment renders them suitable for a wide

**Table 1** Comparison among four types of fibrillar scaffolds: (i) insoluble micro/nanofibrillar scaffolds, (ii) hydrogel nanofibrillar scaffolds based on crystalline cellulose (i.e., bacterial cellulose), (iii) hydrogel nanofibrillar scaffolds based on partially precipitated PVA, and (iv) hydrogel nanofibrillar scaffolds based on chemically cross-linked PVA

Fibrillar type	Composition	Controllability	Fiber stiffness	Transparency
Water-insoluble solid	PCL, PS, PSF, PAN, and so on	Fiber geometry*	High	Low
Crystalline cellulose hydrogel	Bacterial cellulose	N.A.	Intermediate	Intermediate
Partially precipitated hydrogel	PVA	Fiber geometry*, swelling ratio	Low	High
Chemically cross-linked hydrogel	PVA	Fiber geometry*, swelling ratio	Low	High

\*Fiber diameter and density can be controlled via electrospinning

range of applications [53, 54]. Among the abovementioned polymer fibers, the micro/nanofibers based on PCL or PCL-mixed biopolymers are considered one of the most promising cell culture scaffolds. PCL fibers are not only favorable for cell adhesion but also water-stable for a short time and eventually degradable under physiological conditions [13, 55–57]. Moreover, fibrillar scaffolds with appropriate porosity and water wettability can offer a model platform suitable for neurobiological studies. Kim et al. [26] performed dissociated primary cultures of embryonic rat hippocampal neurons on electrospun PS microfiber scaffolds with various fiber diameters and densities (Fig. 1a, b). Furthermore, considering that conventional electrospinning cannot generate micro/nanofibrillar scaffolds that possess both sufficient fiber density and large porosity for cell seeding and cell inclusion, respectively, inside the scaffold as well as vertical neurite outgrowth, we introduced microbead-incorporated micro/nanofibrillar scaffolds composed of solid PS to achieve the two goals mentioned above simultaneously (Fig. 1c). Indeed, the polylysine-modified fiber surface and the large voids among microfibers permitted good neuronal cell adhesion and neurite penetration through the scaffold, respectively (Fig. 1d), while the fine tuning of the fiber geometry permitted the delicate modulation of neurite outgrowth (Fig. 1e, f). In particular, the demonstration of 3D-connected brain cell networks successfully showed the potential of microbead-containing micro/nanofiber scaffolds as a valuable neurobiological culture platform (Fig. 1g–i).

Nonetheless, there still exists room for additional fiber engineering, for example, introducing substructures onto the surface of fibrillar scaffolds for increased effective surface area and/or enhanced molecular diffusion. Moreover, the very low solubility of polymers in water leads to minimal fiber swelling in water, a mechanically stiff solid surface, and the abrupt change in optical refractive index at the water–fiber interface. These phenomena are closely related to the undesirable cellular responses elicited by these scaffolds and their significant light scattering under illumination with visible light (i.e., optical opacity unsuitable for optical microscopy imaging).

## Hydrogel nanofiber network scaffolds based on crystalline bacterial cellulose

BC, which is synthesized by the respiratory process of a microorganism (e.g., *Acetobacter xylinum*), is a nanocrystalline cellulose-based fibrillar network with higher water retention and porosity (1–10  $\mu\text{m}$ ) than conventional plant-derived nanocrystalline cellulose (Fig. 2a) [58, 59]. Furthermore, as shown in Fig. 2a inset and b, BC scaffolds exhibit good optical transparency due to their hydrogel-like properties after the bacterial bodies are removed by NaOH treatment [27]. Therefore, it is reasonable to expect that BC scaffolds will be suitable for various biomedical applications [60]. However, pristine BC scaffolds show uneven surface profiles and 3D unisotropic nanofibrillar superstructures, which could be undesirable for the purpose of 3D cell cultures (Fig. 2c). Therefore, Kim et al. successfully modified natural BC synthesis non-genetically by introducing exogenous carbon nanomaterials into the bacterial culture medium with a proper choice of surfactant and effectively modulated the interactions among the bacteria-synthesized cellulose chains (Fig. 2d) [61].

As depicted in Fig. 2d, the cellulose synthases (i.e., BcsA and BcsB) bound to the bacterial membrane are delicately organized in a linear manner, which enables the alignment for hydrogen bond formation among individual cellulose chains in an aqueous solution [62, 63]. To modify the innate BC structure, the in situ hybridization strategy was successfully exploited in this research. The presence of nanoscale carbon materials such as graphene oxide (GO) nanoflakes disturb the in situ formation of hydrogen bonds among BC chains, thereby weakening the crystallinity of the chains and breaking the helical nanofibrillar orientation (Fig. 2e, f) [27, 64]. Note that because pristine BC exhibits very stable hydrogen bonding, which is extremely hard to alter either chemically or physically, the disruption of BC crystallinity is only possible before the formation of hydrogen bonding among the as-synthesized individual polysaccharide strands spun through the cellulose synthase pores [65]. In comparison with pristine BC, the GO-hybridized BC, which exhibits a well-defined surface profile and structural anisotropy, was successfully employed for

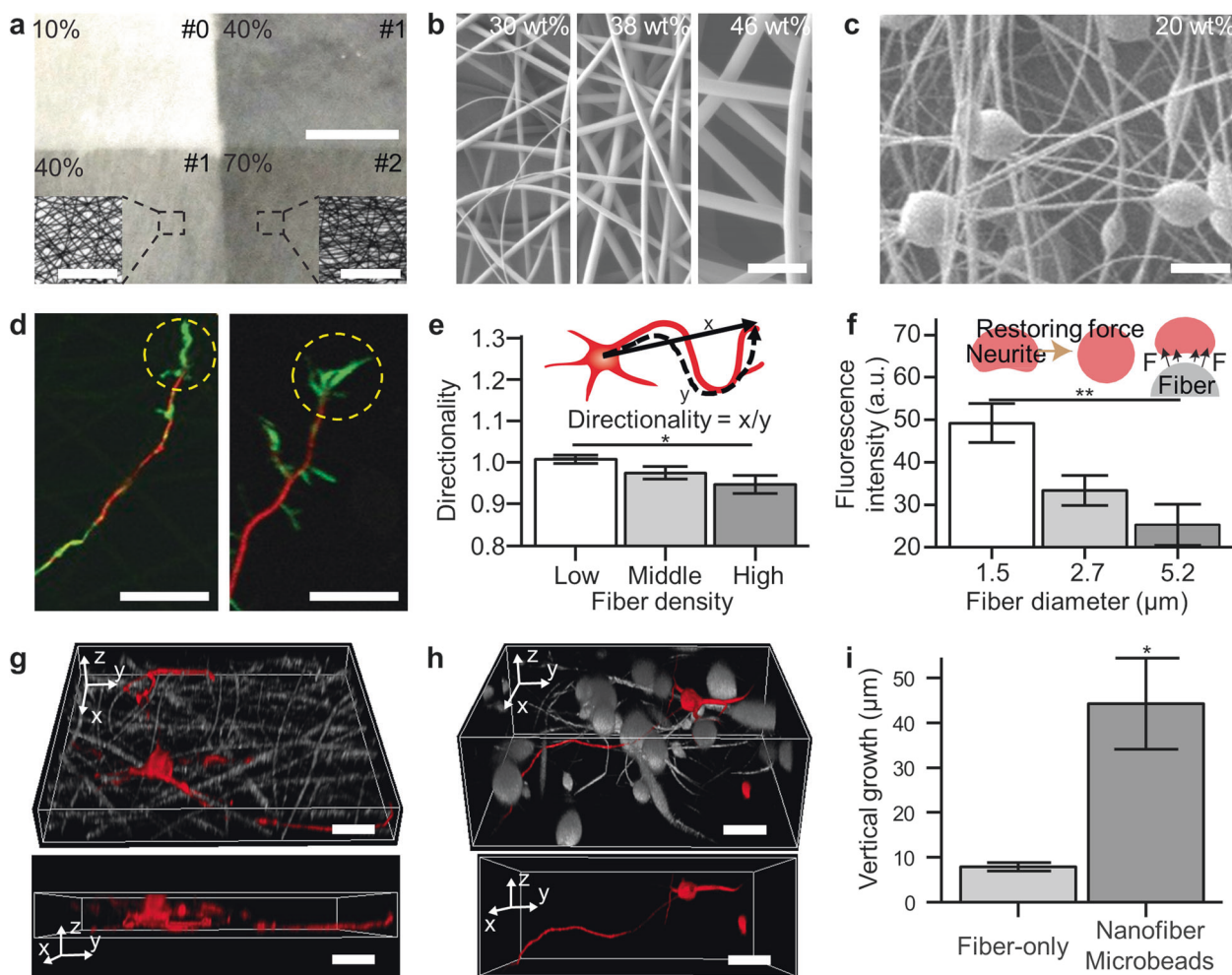


**Fig. 1** **a** Optical micrographs of density-varied electrospun polystyrene (PS) microfibers (scale bar: 500  $\mu\text{m}$ ) and magnified images (inset, scale bar: 100  $\mu\text{m}$ ). **b** Scanning electron microscopy (SEM) images of diameter-controlled electrospun PS fibers (scale bar: 20  $\mu\text{m}$ ). **c** SEM image of microbead-incorporated PS fiber electrospun using a 20 wt% PS precursor solution (scale bar: 20  $\mu\text{m}$ ). **d** Laser-scanning confocal fluorescence microscopy (LSCFM) images of immunostained growth cones of 5-DIV neurons on electrospun PS fibers (left) and a PS culture dish (right) (all scale bars: 20  $\mu\text{m}$ ). **e** Statistical distributions of neuronal directionality (i.e., straightness) at different fiber densities.

The schematic describes the definition of neuronal directionality ( $*p < 0.05$ ). **f** Statistical distributions of fluorescence intensity of immunostained vinculin from 7-DIV neurons cultured on electrospun PS fibers with different fiber diameters ( $*p < 0.01$ ). 3D-reconstructed LSCFM images of 5-DIV neurons cultured on electrospun **g** PS fibers only and on **h** bead-incorporated fibers (all scale bars: 10  $\mu\text{m}$ ). **i** Statistical distributions of vertical neurite growth length on electrospun PS fibers only and on bead-incorporated fibers ( $*p < 0.05$ ). This figure was reproduced from ref. [26]

3D neuronal culture and optically imaged up to the millimeter-depth scale with conventional laser-scanning confocal fluorescence microscopy (LSCFM, Fig. 2g, h).

## Hydrogel micro/nanofiber scaffolds based on partially precipitated PVA

As discussed in the previous section, typical water-insoluble polymer-based fibers show a clear solid–water interface and generally have a hydrophobic surface, leading to optical opacity due to the significant light scattering. In contrast, plant cellulose with hydrophilic functionalities exhibits high

crystallinity and water insolubility due to the strong hydrogen bonding. However, BC, which has specifically arranged cellulose nanofibrillar structures, exhibits both crystallinity and hydrogel-like properties, resulting in optical transparency [58]. Among the various water-soluble polymers, PVA is a simple linear polymer with hydroxyl functionalities. The  $-\text{OH}$  functional groups can be employed for “insoluble” precipitation by thermal annealing-induced hydrogen bonding or “transparent” hydrogel formation by either repeated freeze-thaw cycles or chemical cross-linking with other water-soluble polymers (e.g., alginate) [66]. However, there exist few reports

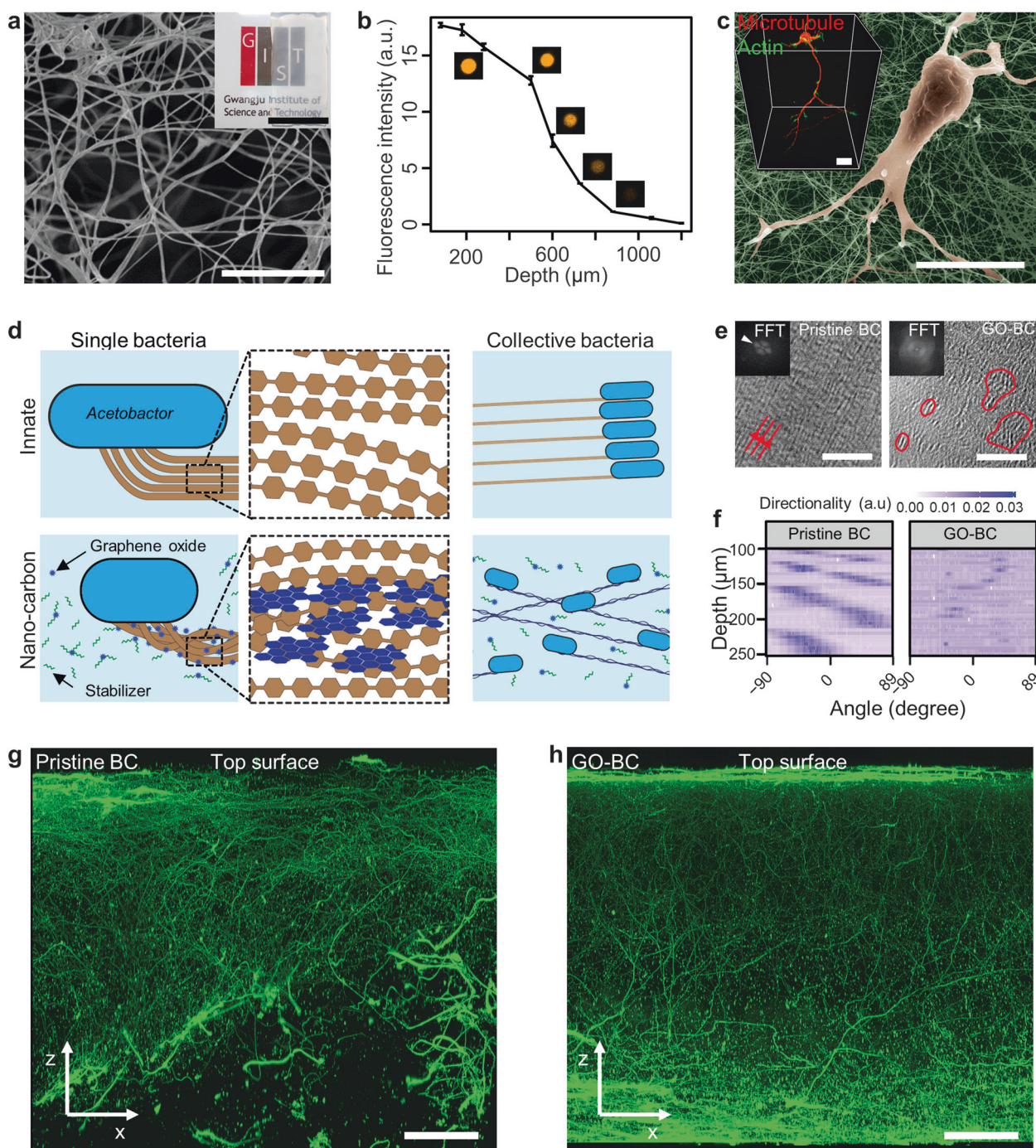


**Fig. 2** **a** SEM (scale bar: 5  $\mu\text{m}$ ) and optical microscopy images (inset, scale bar: 2 cm) of pristine BC. **b** Intensity profiles of fluorescence beads embedded at different depths in pristine BC. **c** SEM and LSCFM (inset) images of 5-DIV neurons cultured on BC (scale bar: 10 and 20  $\mu\text{m}$  for the main and inset images, respectively). **d** Schematic of the non-genetic modulation of bacterial cellulose synthesis without and with exogenous nanomaterials included in the bacterial culture

medium. **e** Transmission electron microscopy (TEM) images of pristine and GO-hybridized BC (all scale bars: 5 nm). **f** Plots of the color-coded frequency of overall nanofibril orientation angle vs. depth in pristine and GO-hybridized BC. **g, h** 3D-reconstructed LSCFM images of tuji1-labeled 20-DIV neurons cultured on pristine and GO-hybridized BC (all scale bars: 500  $\mu\text{m}$ ). This figure was reproduced from ref. [27]

addressing a method to mimic the crystalline and hydrogel-like properties of BC while using PVA homopolymers.

Kim et al. [67] developed a new method to construct a PVA nanofiber-based hydrogel. Conventionally, PVA

precipitates can be easily formed via liquid anti-solvent (LAS) precipitation: once PVA is precipitated by adding a poor solvent to the solution of PVA in a good solvent, the precipitated PVA is no longer dissolved by the good solvent

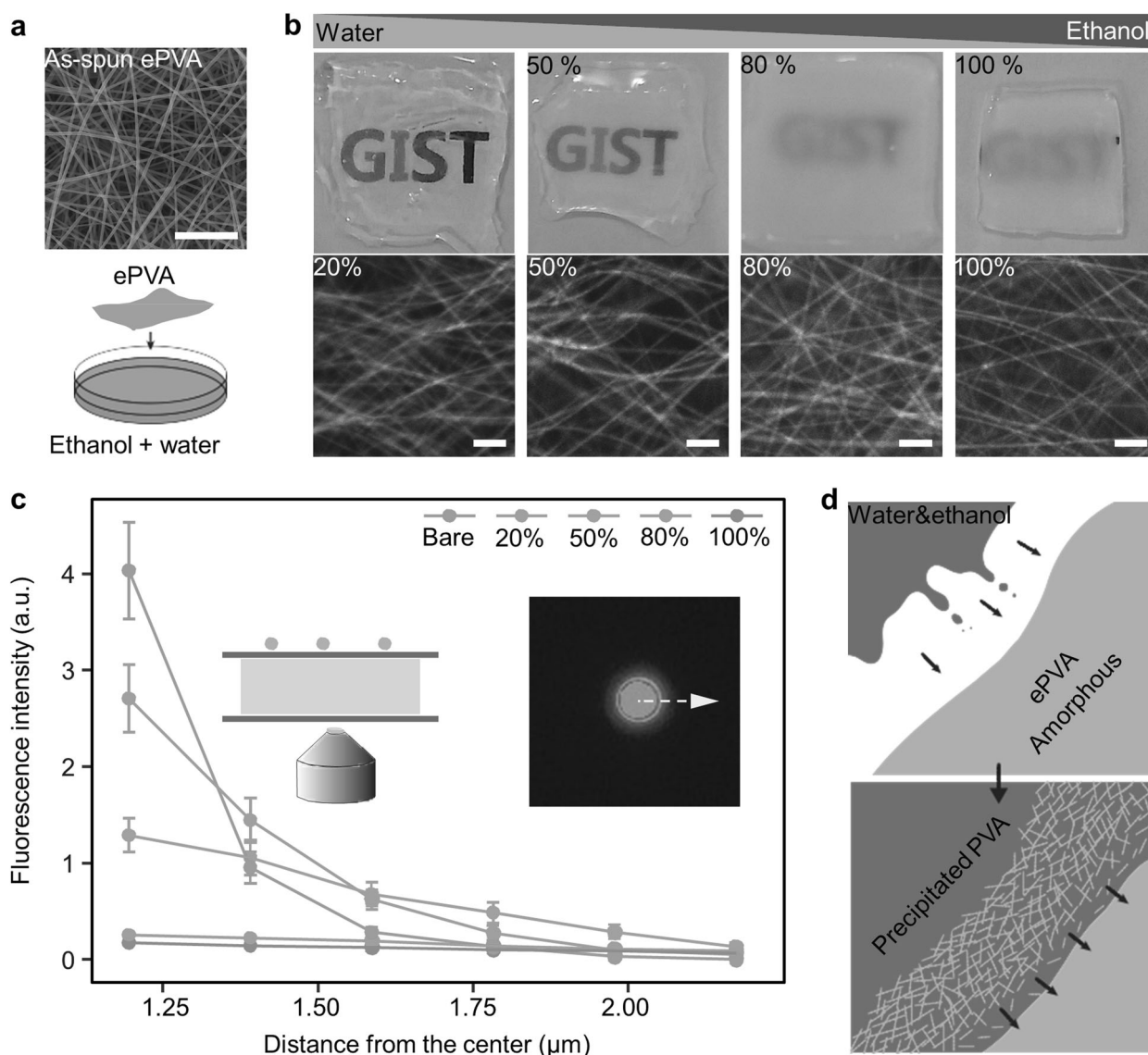


**Fig. 3** **a** SEM image of electrospun polyvinyl alcohol (ePVA) fiber (upper) and schematic of the partial precipitation of ePVA scaffolds via liquid anti-solvent (LAS) precipitation (scale bar: 5  $\mu\text{m}$ ). **b** Optical photographs (upper) and corresponding LSCFM images (below) of wet ePVA prepared with various ethanol concentrations. For fluorescence imaging, wet ePVAs were labeled with calcofluor white (all

scale bars: 5  $\mu\text{m}$ ). **c** Plots of the lateral intensity profiles of fluorescence beads located at the top of various ePVA scaffolds as shown in the schematic (inset). **d** The proposed mechanism of the dynamic LAS process using the ethanol/water mixture. This figure was reproduced from ref. [67]

[68, 69]. Instead, the authors first prepared solid PVA micro/nanofibers and immersed them in a mixture of good (i.e., water) and poor (i.e., ethanol) solvents for hydrogel-like nanofiber formation (Fig. 3a), during which the dissolution (by water) and precipitation (by ethanol) of PVA occur simultaneously at the interface of PVA and the solvent mixture. After dynamic LAS, the optical transparency of the electrospun PVA (ePVA) fibers in the solvent mixture can be enhanced dramatically while still preserving the fibrillar structure by increasing the volume fraction of water in a given water–ethanol mixture. More specifically, Fig. 3b indicates that the greater the fraction of water used in

dynamic LAS, the higher the optical transparency of ePVA. This result suggests that the optical transparency of ePVA in the solvent mixture can be efficiently modulated by the composition of the LAS mixture. To numerically analyze the effect of water content on the optical transparency of the resultant ePVA, fluorescence beads located on top of the solvent mixture-treated ePVA were imaged with an inverted fluorescence microscope. Figure 3c shows the radial intensity profiles of these fluorescent beads in dynamic LAS mixtures at various water contents, indicating that not only enhanced fluorescence intensity (up to  $\sim 10$  times) but also reduced radial broadening that can be observed in ePVA

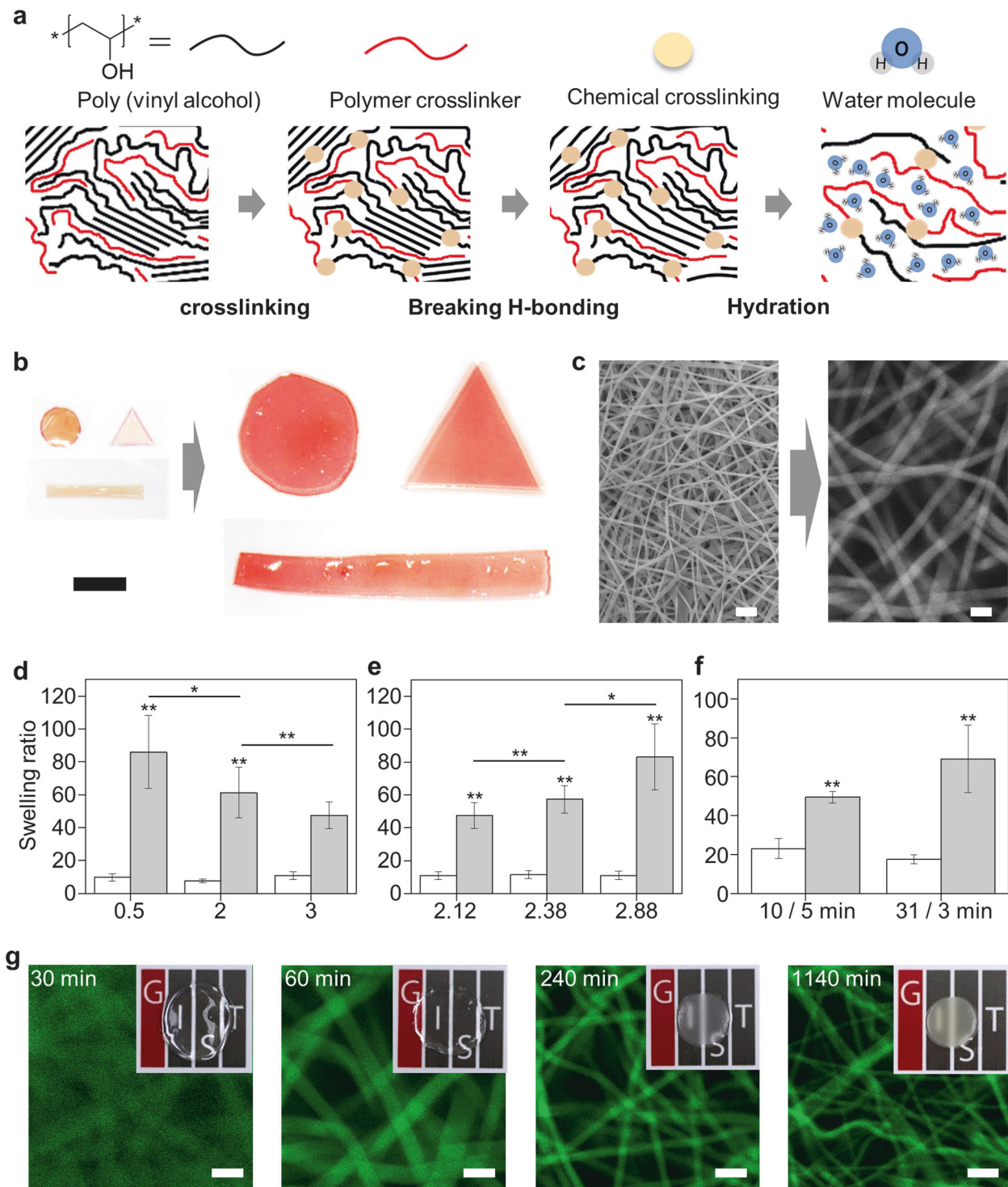


**Fig. 4 a** A schematic of “hydrogelification” using solid-phase electrospun PVA and crosslinkers. **b** Optical images of food-color-stained cross-linked PVA films before (left) and after hydrogelification (right) (scale bar: 1 cm). **c** SEM image of electrospun PVA nanofibrillar scaffolds (left) and LSCFM image of PVA nanofibrillar scaffolds after hydrogelification (right) (all scale bars: 5  $\mu$ m). **d**, **e**, **f** Plots of the swelling ratio of PVA films with (gray columns) and without (white columns) hydrogelification versus the polymer cross-linker

concentration (wt%), the pH of the precursor solution, and the thermal cross-linking reaction time with 10 wt% (left) and 31 wt% (right) cross-linker concentrations. All data are presented with the mean  $\pm$  SD, \* $P < 0.05$  and \*\* $P < 0.001$ . **g** Optical micrographs of wet PVA hydrogel micro/nanofibrillar scaffolds prepared with different cross-linking times at 120  $^{\circ}$ C (all scale bars: 5  $\mu$ m). This figure was reproduced from refs. [70] and [71]

scaffolds treated with dynamic LAS mixtures containing a large amount of water (or a small amount of ethanol). The proposed mechanism is that the water–ethanol mixture can induce the partially swollen PVA to dissolve and subsequently precipitate the amorphous solid as-spun PVA fiber on the surface (Fig. 3d). Furthermore, the relative content of water in the dynamic LAS mixture can determine the extent of swelling and thus the refractive index of the PVA hydrogel-like shell, which is related to the consequent degree of light scattering and the overall optical transparency of the ePVA scaffolds treated with the LAS mixture. We argue that this dynamic process of PVA dissolution and precipitation, which are related to the molecular interactions with good and poor solvents, respectively, continuously occurs at the surface of solid ePVA and that the increase in ethanol content increases the degree of partial precipitation, during which the individual PVA chains are partly connected via hydrogen bonding.

### Hydrogel micro/nanofiber scaffolds based on chemically cross-linked PVA

Typical hydrogels are prepared in the bulk form by carrying out thermal or photocross-linking reactions in a solution of one or two polymer(s). Therefore, it is not straightforward to fabricate hydrogel micro/nanofibers in this manner, as it is difficult to control the reaction sites for chemical cross-linking in the solution phase. Recently, Kang et al. [70] developed a unique method for forming PVA hydrogels by chemical cross-linking in the solid state followed by swelling in water (hydrogelification). As shown in Fig. 4a, the hydrogelification of electrospun micro/nanofibers requires three separate steps: (i) thermal cross-linking in the solid state, (ii) cleavage of hydrogen bonds, and (iii) swelling in water [71] (hydration). This method enables the fabrication of geometry-controlled hydrogels, i.e., film and micro/nanofiber hydrogels with defined shapes and geometric parameters (Fig. 4b, c). Thus far, we have introduced two different types of hydrogel micro/nanofibers in this review. The hydrogel micro/nanofiber scaffolds based on chemically cross-linked polymer are composed of only a hydrogel and a void (i.e., water), while the hydrogel micro/nanofibers based on BC or partially precipitated ePVA contain the crystallized/precipitated solid core of the given polymer fiber other than voids (water). This means that unlike the hydrogels consisting of BC and partially precipitated PVA, hydrogel micro/nanofibers prepared via chemical cross-linking can be formed without hydrogen bond formation.

According to the Flory–Rehner theory, low cross-linking means high swelling, implying that the resultant swelling ratio can be controlled by adjusting the density and degree of chemical cross-linking [33]. Indeed, as shown in

Fig. 4d–f, the apparent swelling ratio of PVA hydrogel micro/nanofiber scaffolds can be easily modulated by controlling the pH, the amount of cross-linking reagent, and the cross-linking reaction time. Furthermore, a series of optical and LSCFM images verify the optical transparency and the geometrical information of hydrogel micro/nanofibers in the aqueous environment (Fig. 4g). It is noteworthy that the fibrillar structures of the hydrogel were well maintained regardless of the specific conditions of hydrogelification, whereas the diameters of the hydrogel micro/nanofibers could be varied by altering the duration of the thermal cross-linking reaction and therefore the cross-linking degree. Furthermore, atomic force microscopy measurements in a liquid cell confirmed that the Young's modulus of a single hydrogel fiber increases with the degree of chemical cross-linking (data not shown). Although the whole mechanical properties of the hydrogel micro/nanofiber cannot be fully represented by the Young's modulus measured from a single fiber, this result suggests that it is possible to perform fundamental studies on the role of mechanical stiffness of hydrogel micro/nanofibers in the behaviors of cells cultured on them because the average modulus and diameter of hydrogel micro/nanofibers based on chemically cross-linked polymers can be fine-tuned by controlling the hydrogelification conditions as described above.

### Conclusions

In this article, we reviewed the recent development in micro/nanofibrillar scaffolds with a specific focus on their biomedical applications. From the perspective of controlling polymer–polymer and polymer–water molecular interactions, we categorized the fibrillar scaffolds into insoluble, nanocrystalline, and hydrogel fibers. Based on our recent research related to this topic, we provide the significance and essential information on four different micro/nanofibrillar scaffolds: (1) solid micro/nanofibrillar scaffolds based on water-insoluble polymers, (2) hydrogel nanofibrillar network scaffolds based on crystalline BC, (3) hydrogel micro/nanofiber scaffolds based on partially precipitated PVA, and (4) hydrogel micro/nanofiber scaffolds based on chemically cross-linked PVA. Solid fiber scaffolds, which are typically composed of water-insoluble synthetic polymers, have been frequently used for many different biomedical applications owing to their large-area porous network structure and aqueous stability. Although PS and PCL micro/nanofibrillar scaffolds have shown potential as versatile biological platforms, their poor optical accessibility and mechanical rigidity have led many researchers to explore hydrogel-like fibrillar scaffolds. Recently, BC, which exhibits high water swelling compared



to plant-derived cellulose, has been recognized as a model nanofibrillar scaffold with hydrogel characteristics. To take advantage of both solid fibers and hydrogel-like BC, micro/nanofibrillar scaffolds based on PVA were proposed as a promising candidate. Since PVA is water-soluble, precipitable, and cross-linkable, leading to the fine control over polymer-to-polymer and polymer-to-water molecular interactions, essential hydrogel characteristics can be realized using PVA by either partial precipitation or solid-state cross-linking in combination with hydration (hydrogelification). We demonstrated that both partial precipitation conducted by dynamic LAS and hydrogelification by chemical cross-linking enable the fabrication of hydrogel micro/nanofibers in the solid state. These methods provide optical transparency, geometric/shape control, and subtle modulation of swelling; thus, mechanical properties that would open new opportunities for various high-impact applications in the field of biomedical engineering can be realized.

**Acknowledgements** This research was supported by National R&D Program through the National Research Foundation of Korea (NRF) funded by the Ministry of Science, ICT and Future Planning (NRF-2012-0009664), and GIST Research Institute (GRI) grant funded by the GIST in 2018.

### Compliance with ethical standards

**Conflict of interest** The authors declare that they have no conflict of interest.

### References

- Kim C, Park S-H, Lee W-J, Yang K-S. Characteristics of supercapacitor electrodes of PBI-based carbon nanofiber web prepared by electrospinning. *Electrochim Acta*. 2004;50:877–81.
- Kim JR, Choi SW, Jo SM, Lee WS, Kim BC. Electrospun PVdF-based fibrous polymer electrolytes for lithium ion polymer batteries. *Electrochim Acta*. 2004;50:69–75.
- Schechner P, Kroll E, Bubis E, Chervinsky S, Zussman E. Silver-plated electrospun fibrous anode for glucose alkaline fuel cells. *J Electrochem Soc*. 2007;154:B942–8.
- Subramania A, Devi SL. Polyaniline nanofibers by surfactant-assisted dilute polymerization for supercapacitor applications. *Polym Adv Technol*. 2008;19:725–7.
- Li M, Zhao S, Han G, Yang B. Electrospinning-derived carbon fibrous mats improving the performance of commercial Pt/C for methanol oxidation. *J Power Sources*. 2009;191:351–6.
- Jung J-W, Lee C-L, Yu S, Kim I-D. Electrospun nanofibers as a platform for advanced secondary batteries: a comprehensive review. *J Mater Chem A*. 2016;4:703–50.
- Gopal R, Kaur S, Ma Z, Chan C, Ramakrishna S, Matsuura T. Electrospun nanofibrous filtration membrane. *J Membr Sci*. 2006;281:581–6.
- Gopal R, Kaur S, Feng CY, Chan C, Ramakrishna S, Tabe S, Matsuura T. Electrospun nanofibrous polysulfone membranes as pre-filters: particulate removal. *J Membr Sci*. 2007;289:210–9.
- Li H-W, Wu C-Y, Tepper F, Lee J-H, Lee CN. Removal and retention of viral aerosols by a novel alumina nanofiber filter. *J Aerosol Sci*. 2009;40:65–71.
- Xue J, He M, Liang Y, Crawford A, Coates P, Chen D, Shi R, Zhang L. Fabrication and evaluation of electrospun PCL–gelatin micro-/nanofiber membranes for anti-infective GTR implants. *J Mater Chem B*. 2014;2:6867–77.
- Yoshimoto H, Shin YM, Terai H, Vacanti JP. A biodegradable nanofiber scaffold by electrospinning and its potential for bone tissue engineering. *Biomaterials*. 2003;24:2077–82.
- Czaja W, Krystynowicz A, Bielecki S, Brown RM. Microbial cellulose—the natural power to heal wounds. *Biomaterials*. 2006;27:145–51.
- Xie J, Willerth SM, Li X, Macewan MR, Rader A, Sakiyama-Elbert SE, Xia Y. The differentiation of embryonic stem cells seeded on electrospun nanofibers into neural lineages. *Biomaterials*. 2009;30:354–62.
- Xie J, MacEwan MR, Schwartz AG, Xia Y. Electrospun nanofibers for neural tissue engineering. *Nanoscale*. 2010;2:35–44.
- Wang C, Yan K-W, Lin Y-D, Hsieh PCH. Biodegradable core/shell fibers by coaxial electrospinning: processing, fiber characterization, and its application in sustained drug release. *Macromolecules*. 2010;43:6389–97.
- Liu W, Thomopoulos S, Xia Y. Electrospun nanofibers for regenerative medicine. *Adv Healthcare Mater*. 2012;1:10–25.
- Huang Z-M, Zhang Y-Z, Kotaki M, Ramakrishna S. A review on polymer nanofibers by electrospinning and their applications in nanocomposites. *Compos Sci Technol*. 2003;63:2223–53.
- Zhang S. Fabrication of novel biomaterials through molecular self-assembly. *Nat Biotechnol*. 2003;21:nbt874.
- Raghvendra KM, Sravanthi L. Fabrication techniques of micro/nano fibres based nonwoven composites: a review. *Mod Chem Appl*. 2017;5:1–11.
- Li D, Xia Y. Direct fabrication of composite and ceramic hollow nanofibers by electrospinning. *Nano Lett*. 2004;4:933–8.
- McCann JT, Marquez M, Xia Y. Highly porous fibers by electrospinning into a cryogenic liquid. *J Am Chem Soc*. 2006;128:1436–7.
- Lu P, Xia Y. Maneuvering the internal porosity and surface morphology of electrospun polystyrene yarns by controlling the solvent and relative humidity. *Langmuir*. 2013;29:7070–8.
- Mashayekhan S, Hajiabbas M, Fallah A. Stem cells in tissue engineering. *Pluripotent Stem Cells*. 2013. <https://doi.org/10.5772/54371>.
- Wei K, Kim I-S. Fabrication of nanofibrous scaffolds by electrospinning. *Advances in Nanofibers*. 2013. <https://doi.org/10.5772/57093>.
- Wu J, Hong Y. Enhancing cell infiltration of electrospun fibrous scaffolds in tissue regeneration. *Bioact Mater*. 2016;1:56–64.
- Kim D, Kim S-M, Lee S, Yoon M-H. Investigation of neuronal pathfinding and construction of artificial neuronal networks on 3D-arranged porous fibrillar scaffolds with controlled geometry. *Sci Rep*. 2017;7:7716.
- Kim D, Park S, Jo I, Kim S-M, Kang DH, Cho S-P, Park JB, Hong BH, Yoon M-H. Multiscale modulation of nanocrystalline cellulose hydrogel via nanocarbon hybridization for 3D neuronal bilayer formation. *Small*. 2017;13:1700331.
- Wang X, Ding B, Li B. Biomimetic electrospun nanofibrous structures for tissue engineering. *Mater Today*. 2013;16:229–41.
- Baker BM, Trappmann B, Wang WY, Sakar MS, Kim IL, Shenoy VB, Burdick JA, Chen CS. Cell-mediated fibre recruitment drives extracellular matrix mechanosensing in engineered fibrillar microenvironments. *Nat Mater*. 2015;14:1262–8.
- Caló E, Khutoryanskiy VV. Biomedical applications of hydrogels: a review of patents and commercial products. *Eur Polym J*. 2015;65:252–67.

31. Fernandez-Yague MA, Abbah SA, McNamara L, Zeugolis DI, Pandit A, Biggs MJ. Biomimetic approaches in bone tissue engineering: Integrating biological and physicochemical strategies. *Adv Drug Deliv Rev.* 2015;84:1–29.
32. Drury JL, Mooney DJ. Hydrogels for tissue engineering: scaffold design variables and applications. *Biomaterials.* 2003;24:4337–51.
33. Slaughter BV, Khurshid SS, Fisher OZ, Khademhosseini A, Peppas NA. Hydrogels in regenerative medicine. *Adv Mater.* 2009;21:3307–29.
34. Vining KH, Mooney DJ. Mechanical forces direct stem cell behaviour in development and regeneration. *Nat Rev Mol Cell Biol.* 2017;18:728.
35. Helvert S, van, Storm C, Friedl P. Mechanoreciprocity in cell migration. *Nat Cell Biol.* 2018;20:8–20.
36. Varghese JS, Chellappa N, Fathima NN. Gelatin–carrageenan hydrogels: role of pore size distribution on drug delivery process. *Colloids Surf B Biointerfaces.* 2014;113:346–51.
37. Ishikiriya K, Sakamoto A, Todoki M, Tayama T, Tanaka K, Kobayashi T. Pore size distribution measurements of polymer hydrogel membranes for artificial kidneys using differential scanning calorimetry. *Thermochim Acta.* 1995;267:169–80.
38. Annabi N, Tamayol A, Uquillas JA, Akbari M, Bertassoni LE, Cha C, Camci-Unal G, Dokmeci MR, Peppas NA, Khademhosseini A. 25th Anniversary article: rational design and applications of hydrogels in regenerative medicine. *Adv Mater.* 2014;26:85–124.
39. Thiele J, Ma Y, Bruekers SMC, Ma S, Huck WTS. 25th Anniversary article: designer hydrogels for cell cultures: a materials selection guide. *Adv Mater.* 2014;26:125–48.
40. Choi SH, Kim YH, Hebisch M, Sliwinski C, Lee S, D'Avanzo C, Chen H, Hooli B, Asselin C, Muffat J, Klee JB, Zhang C, Wainger BJ, Peitz M, Kovacs DM, Woolf CJ, Wagner SL, Tanzi RE, Kim DY. A three-dimensional human neural cell culture model of Alzheimer's disease. *Nature.* 2014;515:274–8.
41. Liu L, You Z, Yu H, Zhou L, Zhao H, Yan X, Li D, Wang B, Zhu L, Xu Y, Xia T, Shi Y, Huang C, Hou W, Du Y. Mechanotransduction-modulated fibrotic microniches reveal the contribution of angiogenesis in liver fibrosis. *Nat Mater.* 2017. <https://doi.org/10.1038/nmat5024>.
42. Knight E, Przyborski S. Advances in 3D cell culture technologies enabling tissue-like structures to be created in vitro. *J Anat.* 2015;227:746–56.
43. Darnell M, Mooney DJ. Leveraging advances in biology to design biomaterials. *Nat Mater.* 2017;16:1178.
44. Roach P, Parker T, Gadegaard N, Alexander MR. Surface strategies for control of neuronal cell adhesion: a review. *Surf Sci Rep.* 2010;65:145–73.
45. Woodruff MA, Hutmacher DW. The return of a forgotten polymer—polycaprolactone in the 21st century. *Prog Polym Sci.* 2010;35:1217–56.
46. Zheng J, He A, Li J, Xu J, Han CC. Studies on the controlled morphology and wettability of polystyrene surfaces by electrospinning or electrospraying. *Polymer.* 2006;47:7095–102.
47. Casper CL, Stephens JS, Tassi NG, Chase DB, Rabolt JF. Controlling surface morphology of electrospun polystyrene fibers: effect of humidity and molecular weight in the electrospinning process. *Macromolecules.* 2004;37:573–8.
48. Nabe A, Staude E, Belfort G. Surface modification of polysulfone ultrafiltration membranes and fouling by BSA solutions. *J Membr Sci.* 1997;133:57–72.
49. Prince JA, Singh G, Rana D, Matsuura T, Anbharasi V, Shanmugasundaram TS. Preparation and characterization of highly hydrophobic poly(vinylidene fluoride) – clay nanocomposite nanofiber membranes (PVDF–clay NNMs) for desalination using direct contact membrane distillation. *J Membr Sci.* 2012;397–398:80–6.
50. Rana D, Singh G, Prince JA, Ayyanar N, Matsuura T, Shanmugasundaram TS. Nanofiber based triple layer hydro-philic/-phobic membrane - a solution for pore wetting in membrane distillation. *Sci Rep.* 2014;4:6949.
51. Feng L, Li S, Li H, Zhai J, Song Y, Jiang L, Zhu D. Superhydrophobic surface of aligned polyacrylonitrile nanofibers. *Angew Chem.* 2002;114:1269–71.
52. Feng C, Khulbe KC, Matsuura T, Tabe S, Ismail AF. Preparation and characterization of electro-spun nanofiber membranes and their possible applications in water treatment. *Sep Purif Technol.* 2013;102:118–35.
53. Xu H, Cai S, Sellers A, Yang Y. Intrinsically water-stable electrospun three-dimensional ultrafine fibrous soy protein scaffolds for soft tissue engineering using adipose derived mesenchymal stem cells. *RSC Adv.* 2014;4:15451–7.
54. Xu H, Cai S, Xu L, Yang Y. Water-stable three-dimensional ultrafine fibrous scaffolds from keratin for cartilage tissue engineering. *Langmuir.* 2014;30:8461–70.
55. Schnell E, Klinkhammer K, Balzer S, Brook G, Klee D, Dalton P, Mey J. Guidance of glial cell migration and axonal growth on electrospun nanofibers of poly-ε-caprolactone and a collagen/poly-ε-caprolactone blend. *Biomaterials.* 2007;28:3012–25.
56. Vaz CM, van Tuijl S, Bouten CVC, Baaijens FPT. Design of scaffolds for blood vessel tissue engineering using a multi-layering electrospinning technique. *Acta Biomater.* 2005;1:575–82.
57. Gupta D, Venugopal J, Prabhakaran MP, Dev VRG, Low S, Choon AT, Ramakrishna S. Aligned and random nanofibrous substrate for the in vitro culture of Schwann cells for neural tissue engineering. *Acta Biomater.* 2009;5:2560–9.
58. Klemm D, Heublein B, Fink H-P, Bohn A. Cellulose: fascinating and sustainable raw material. *Angew Chem Int Ed Engl.* 2005;44:3358–93.
59. Cheng S, Zhang Y, Cha R, Yang J, Jiang X. Water-soluble nanocrystalline cellulose films with highly transparent and oxygen barrier properties. *Nanoscale.* 2016;8:973–8.
60. Cacicedo ML, Castro MC, Servetas I, Bosnea L, Boura K, Tsafrikidou P, Dima A, Terpou A, Koutinas A, Castro GR. Progress in bacterial cellulose matrices for biotechnological applications. *Bioresour Technol.* 2016;213:172–80.
61. Haigler CH, White AR, Brown RM, Cooper KM. Alteration of in vivo cellulose ribbon assembly by carboxymethylcellulose and other cellulose derivatives. *J Cell Biol.* 1982;94:64–9.
62. Mehta K, Pfeffer S, M. B. R Jr. Characterization of an acsD disruption mutant provides additional evidence for the hierarchical cell-directed self-assembly of cellulose in *Gluconacetobacter xylinus*. *Cellulose.* 2014;22:119–37.
63. Deng Y, Nagachar N, Fang L, Luan X, Catchmark JM, Tien M, Kao T. Isolation and characterization of two cellulose morphology mutants of *Gluconacetobacter hansenii* ATCC23769 producing cellulose with lower crystallinity. *PLoS ONE.* 2015;10:e0119504.
64. Park S, Park J, Jo I, Cho S-P, Sung D, Ryu S, Park M, Min K-A, Kim J, Hong S, Hong BH, Kim B-S. In situ hybridization of carbon nanotubes with bacterial cellulose for three-dimensional hybrid bioscaffolds. *Biomaterials.* 2015;58:93–102.
65. Haigler CH, Brown RM, Benziman M. Calcofluor white ST alters the in vivo assembly of cellulose microfibrils. *Science.* 1980;210:903–6.
66. Baker MI, Walsh SP, Schwartz Z, Boyan BD. A review of polyvinyl alcohol and its uses in cartilage and orthopedic applications. *J Biomed Mater Res B Appl Biomater.* 2012;100B:1451–7.
67. Kim D, Kang D-H, Wang S, Hung TT, Lee W-J, Kim S-M, Kim J-A, Yoon M-H. Fabrication of fibrillary hydrogel scaffold via

- liquid antisolvent process for three-dimensional neuronal network construction (submitted).
68. Thorat AA, Dalvi SV. Liquid antisolvent precipitation and stabilization of nanoparticles of poorly water soluble drugs in aqueous suspensions: recent developments and future perspective. *Chem Eng J.* 2012;181–182:1–34.
  69. Zhao H, Wang J-X, Wang Q-A, Chen J-F, Yun J. Controlled liquid antisolvent precipitation of hydrophobic pharmaceutical nanoparticles in a microchannel reactor. *Ind Eng Chem Res.* 2007;46:8229–35.
  70. Kang D-H, Song D, Lee W-J, Wang S, Goh M, Tae G, Yoon M-H. A new approach to hydrogel formation based on solid state polyvinyl alcohol: hydrogelification (submitted).
  71. Kang D-H, Wang S, Kim D, Song D, Yoon M-H. Novel class of polyvinyl alcohol-based nanofiber for a controllable cell culture platform (in preparation).